Наносистеми, наноматеріали, нанотехнології
Nanosistemi, Nanomateriali, Nanotehnologii
2025, т. 23, № 4, сс. 1041–1057
https://doi.org/10.15407/nnn.23.04.1041

PACS numbers: 62.20.Qp, 62.25.Mn, 68.35.bj, 68.37.Hk, 68.70.+w, 81.05.Pj, 87.85.Rs

The Mechanism of Nucleation in Glass-Ceramic Materials Based on Lithium Disilicate with Increased Fracture Toughness

O. V. Savvova[1], I. V. Yanishyn[2], O. I. Fesenko[1], O. L. Fedotova[2], O. V. Babich[1], Yu. O. Smyrnova[1], and D. A. Bulavina[1]

[1]*O. M. Beketov National University of Urban Economy in Kharkiv, 17, Chornoglazivska Str., UA-61002 Kharkiv, Ukraine*
[2]*Kharkiv National Medical University, 4, Nauky Ave., UA-61022 Kharkiv, Ukraine*

Innovative directions for the development of new types of competitive materials for dentistry are analysed to solve important social problems related to improving the quality of life of people and emergency care in crisis situations. A comparative assessment of the properties and areas of application of commercial dental materials is carried out and the prospects for the use of glass-ceramic materials based on lithium disilicate for solving problems of long-term functionality are determined. The criteria, which determine the formation of a high-strength sitallized nanostructure of the glass matrix and ensure the necessary properties of the glass-ceramic material under low-temperature synthesis conditions, are selected. Glass compositions are developed and the character of their crystallization is studied. The mechanism of nucleation and the conditions for the formation of the dendritic structure of experimental glasses during heat treatment are determined. The operational properties of the developed glass-ceramic materials are studied and the possibility of obtaining competitive materials, in accordance with DIN EN ISO 13485, with increased fracture toughness $K_{1C} = 5.0$ MPa·m$^{1/2}$ is established.

Проаналізовано інноваційні напрями розвитку нових видів конкурентоспроможних матеріялів для стоматології задля вирішення важливих соціяльних задач щодо поліпшення якости життя людей і невідкладної допомоги у кризових ситуаціях. Проведено порівняльну оцінку властивостей та областей застосування комерційних стоматологічних матеріялів і визначено перспективність застосування склокристалічних матеріялів на основі дисилікату Літію для вирішення проблем довгострокової функціональности. Обрано критерії, за якими визначають формування високоміцної ситалізованої наноструктури скломатриці та забезпечення

потрібних властивостей склокристалічного матеріялу в умовах низькотемпературної синтези. Розроблено склади стекол і досліджено характер їхньої кристалізації. Визначено механізм зародкоутворення й умови формування дендритної структури дослідних стекол у процесі термічного обробляння. Досліджено експлуатаційні властивості розроблених склокристалічних матеріялів і встановлено можливість одержання конкурентоздатних матеріялів у відповідності до DIN EN ISO 13485 з підвищеними показниками тріщиностійкости $K_{1C}=5{,}0$ МПа·м$^{1/2}$.

Key words: glass-ceramic materials, lithium disilicate, nanostructure, dendritic structure, fracture toughness, dentistry.

Ключові слова: склокристалічні матеріяли, дисилікат Літію, наноструктура, дендритна структура, тріщиностійкість, стоматологія.

(Received 10 January, 2025)

1. INTRODUCTION

Today, the intensive development of dental prosthetics determines the need for the development and use of a wide range of materials, among which oxide ceramic materials and glass materials based on silicates with high physicochemical and biological properties, which are capable of creating a single cellular and material structure in the body [1], occupy the leading place. Innovative directions in the development of new types of materials for dentistry are associated with the creation of new competitive prostheses, which will differ, when compared with well-known brands, in a combination of high operational and technological properties and at the same time reduced cost. Among foreign manufacturing companies, ceramic and glass materials [2] of the following companies deserve special attention: Ivoclar Vivadent IPS Empress; EstheticIPS; EmpressIPS e.max Ceram; Harmony; d.SIGN; Callisto Implant; Callisto Implant; Callisto Pd; Brite Gold XH; d.SIGN, *etc.*, which are widely used in dental prosthetics. Commercial products Procera™ AllCeram (Al_2O_3), ITA In-Ceram® YZ (5Y-TZP), Vita Mark II (Feldspar glass-ceramic), ProCAD (Leucite-reinforced glass-ceramic), IPS e.max CAD (lithium disilicate glass-ceramic) today occupy a significant part of the dental ceramic market (Fig. 1). However, these materials are characterized by high cost and cannot be used to solve important social problems related to improving the quality of life of all segments of the population, especially emergency care in crisis situations, when the demand for high-quality affordable dental materials is significantly increasing.

For a long time, the practically available ceramic material used in medicine for dental prosthetics was porcelain, which has high cos-

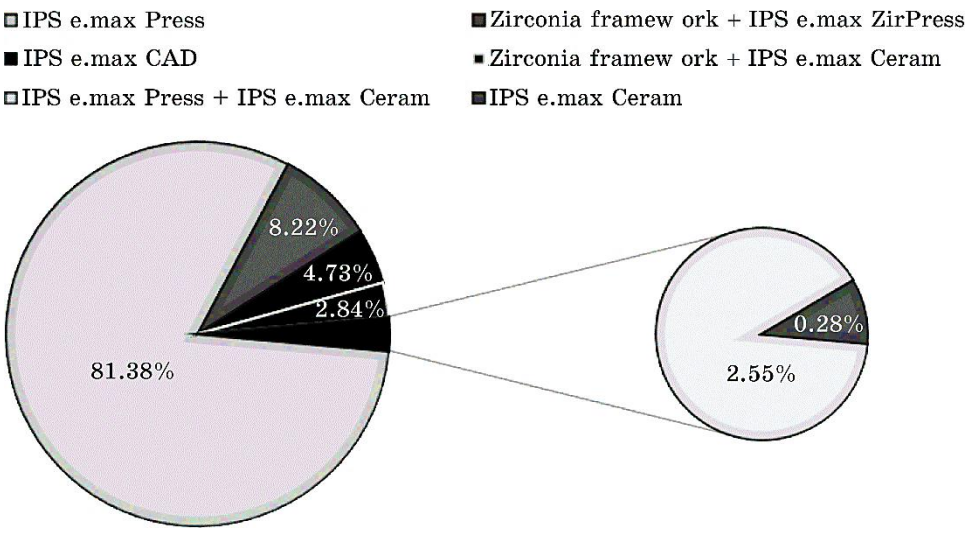

Fig. 1. Distribution of the frequency of use of restorative materials.

metic characteristics, but is characterized by low mechanical properties. Dental porcelain is synthesized on the base of feldspar in the $K_2O–Al_2O_3–SiO_2$ system [2]. For example, the compressive strength of modern porcelain EX-3 Hopumaku (Kuraray Noritake, Japan) is 100–110 MPa (according to ISO 9693 it should be at least 50 MPa). However, the wear resistance and physical and mechanical characteristics of such prostheses, in some cases, do not meet the requirements of standards for dental implants, which are subjected to significantly higher mechanical loads during chewing. This does not allow the use of dental porcelain for the manufacture of solid dental crowns. In this case, oxide or composite ceramics are successfully used.

High-density, high-purity ceramics based on α-Al_2O_3 were the first ceramic material widely used in medicine, in particular, for the manufacture of femoral head prostheses and dental implants, due to its exceptional corrosion resistance, biocompatibility, low friction resistance, high wear resistance and strength [3] (Table 1). The high hardness and high melting point of aluminium oxide complicate the technological process of manufacturing individual structures in dentistry.

Zirconia-based materials are commonly used in dentistry due to their good mechanical characteristics and aesthetic appeal. However, it is necessary to improve their biological response for practical application in clinical settings [4]. Zirconium dioxide is designed for use under high load conditions and is characterized by high resistance to fatigue fracture stress, which is extremely important

TABLE 1. Characteristics of the main properties of the most common silicate materials for prosthetics [2].

Material	Ceramic type (chemical components)	Flexural strength, MPa	Modulus of elasticity, GPa	Vickers hardness, GPa	Fracture toughness, $MPa \cdot m^{1/2}$	Use
Al_2O_3	Al_2O_3	784.8–1953.5*	—	17.90–18.90	3.50–4.90	Single crown
Zirconia stabilized with yttrium oxide	5Y-TZP	665–2374*	200–210	12.65–13.43	5.90	Single-crown and three-unit anterior and posterior bridge
Feldspar glass-ceramics	SiO_2, Al_2O_3, Na_2O, K_2O, CaO, TiO_2	154	45	5.75–6.19	1.16–1.66	Veneers, inlays, onlays, partial crowns, anterior and posterior crowns, CAD/CAM material
Leucite-reinforced glass-ceramics	SiO_2, BaO, Al_2O_3, CaO, CeO_2, Na_2O, K_2O, B_2O_3, TiO_2	160	62	1.66–1.88	1.17–1.69	
Lithium disilicate glass-ceramics	SiO_2, Li_2O, K_2O, P_2O_5, ZrO_2, ZnO, Al_2O_3, MgO	320–400	95	6.68–7.00	1.95–2.41	The same three-unit bridges (anterior and premolar), hybrid abutments, hybrid abutment crowns

*Fracture strength, N.

when creating dental materials that are used under conditions of significant repeatedly variable loads [5].

With the advent of CAD/CAM systems (Computer Aided Des-

ing/Computer Aided Manufacture), zirconia-based ceramics have become more widely used [6].

Pure zirconia is found in the monoclinic form at ambient temperature, and when subjected to elevated temperatures (1170°C) or low-temperature degradation, it undergoes a transformation to the tetragonal form [7].

The solution to this problem is the creation of GCM that are distinguished by high performance properties, manufacturability and are less expensive compared to ceramic dental prostheses.

Leucite-containing dental GSM are one of the most promising materials in the manufacture of metal–ceramic crowns for prosthetics of anterior and chewing teeth. The main difference between glass-ceramics and feldspar and lanthanum glass, which have long been used for facing metal–ceramic prostheses, is that the formation of a sitallized structure of glass-ceramics with the presence of leucite crystals up to 1 μm in size evenly distributed in the volume of the material that allows for high strength characteristics of the materials.

Thus, the flexural strength of the material strengthened with leucite is higher than 120 MPa. Adding enstatite to leucite-containing glass-ceramics allows to increase the fracture toughness index to 3.5–4.6 $MPa \cdot m^{1/2}$ [8], and bioactive glass increases the ability to regenerate bone tissue [9].

Machined glass-ceramic materials (GCM) based on mica containing fluorophlogopite ($K_{1-x}Mg_{3-y}Al_y[(A,B)_{1+z}Si_{3+z}O_{10+w}]F_{2-w}$) are known to provide dental prostheses with fluorescent properties similar to natural teeth. A unique variety of these glass-ceramics was developed within the SiO_2–B_2O_3–Al_2O_3–MgO–F system and subsequently marketed under the brand name Macor [10].

The flexural strength of this material is 120–150 MPa, which, combined with high adhesion to hard tooth tissues, is quite sufficient for the manufacture of onlays, veneers or crowns of chewing teeth, but is insufficient for the manufacture of all-ceramic bridges.

One of the most effective commercial materials in dentistry, which has found a wide range of applications in the production of veneers, crowns and fixed dentures up to three units long, is glass-ceramics based on lithium disilicate (LS_2). These dental materials, which can be obtained using traditional glass production technologies and energy-saving technologies (sol–gel) [11], demonstrate high flexural strength of 300–400 MPa, high fracture toughness of 2.8–3.5 $MPa \cdot m^{1/2}$, hardness similar to natural teeth, and high chemical resistance.

The commercial IPS Empress© material paved the way for the growing success of LS_2 GSM in dentistry. The subsequent technical revolution allowed the transition from the pressed IPS e.max©

Press to the computer-aided design/manufacturing (CAD/CAM) IPS e.max© CAD (Fig. 1) [12]. The ability to be easily milled (in the partially crystallized state, materials containing lithium metasilicate crystals) is also crucial, as it simplifies the fabrication methods of the prosthesis and allows for delocalization of production.

The authors [13] improved the composition of IPS e.max CAD, which is as follows: 57–80% SiO_2, 11–19% Li_2O, 0–13% K_2O, 0–11% P_2O_5, 0–8% ZrO_2–ZnO, 0–5% Al_2O_3, 0–5% MgO, and colouring oxides and obtained a new glass named LSM CAD. The composition consists of 50–60% SiO_2, 20–30% Li_2O, 0–10% K_2O, 0–10% P_2O_5, 0–5% CaO, 0–5% BaO, 0–5% Al_2O_3, 0–5% MgO, and 0–5% Sb_2O_3. Four distinct nucleation heat treatments were performed: T_1 (500°C, 90 min), T_2 (500°C, 180 min), T_3 (500°C, 360 min), and T_4 (480°C, 360 min). The T_2 and T_4 GCM demonstrated the best properties in comparison to the control group. Notably, although their crystallized fraction was relatively small at approximately 57%, they achieved a hardness ranging from 5.6 to 6.0 GPa, a value that is both adequate and statistically comparable to that of the control group. The same groups achieved BFS values ranging from 270 to 448 MPa and from 346 to 640 MPa. The mechanical properties of the material under investigation were effectively enhanced by adjusting the nucleation temperature and duration, resulting in values that are comparable to, though not exceeding, the flexural strength of the commercial dental GCM IPS e.max CAD, which is 360 MPa, and a Vickers hardness of 5.8 GPa.

Along with the advantages of using GCM as dental prostheses, a significant problem of all commercial glass materials for dental purposes is the low stress intensity coefficient $K_{1C} = 1.39–2.18$ MPa·$m^{1/2}$ (Table 1), which significantly affects the duration of their operation under variable loads.

The authors of [14] developed high-strength GCM based on LS_2 with the marking SL 9-DTs-5, which is strengthened by introducing 5 wt.% of yttrium-stabilized zirconium oxide and transparent GCM with marking SL 12-Z strengthened by ion-exchange treatment in $NaNO_3$ vapours ($T = 550$°C, $\tau = 1$ h), which were obtained under conditions of low-temperature short-term heat treatment (SL 9-DTs-5: stage I—600°C, 2 h; stage II—900°C, 1.5 h; SL 12-Z: stage I—630°C, 0.5 h; stage II—850°C, 0.08 h).

The developed GCM were characterized by the presence of a finely dispersed oriented interlocking structure of the material with the presence of high-strength crystalline phases LS_2 in an amount of 50–85 vol.% and adjustable light transmittance (T) and high mechanical properties (Table 2).

The increase in the crack resistance index for these materials is explained by the formation of nanoscale structure and crack block-

TABLE 2. Characteristics of phase composition and properties of natural teeth and LS_2-based materials [2, 14–18].

Marking	Characteristics of the main crystalline phases		Properties					
	Type	Content, vol.%	*HV*, GPa	K_{1C}, MPa·m$^{1/2}$	*E*, GPa	$\alpha \cdot 10^7$, deg^{-1}	ρ, g/cm^3	*T*, %
Tooth enamel	Dihydroxyapatite, calcium carbonate, calcium fluoride, magnesium phosphate	95.0–97.0	3.30–7.00	1.12–1.35	75–130	—	—	—
IPS e.max CAD	LS_2	64.5	5.80	2.25	95	105	—	—
SL 12-Z	LS_2, β-SP	50.0	11.50	3.25	315	90	2380	—
SL 9-DTs-5	LS_2, ZrO_2	85.0	8.86	12.00	380	63	2450	70

ing due to the structural rearrangement of the material during forming. Research indicates that a specific crystallographic orientation of LS_2 crystals contributes to a reduction in the variability of the material's elastic properties. This orientation results in an elastic modulus reaching up to 307 GPa, a compressive strength of 650 MPa, and an impact strength of as much as 5.5 kJ/mI. It was demonstrated that the formation of a closed-form mesh block structure by 0.4 μm-LS_2 lamellar crystals results in a material with exceptional strength characteristics. Additionally, this material exhibits transparency within the visible light spectrum, enabling its application as a foundational component for the creation of transparent bulletproof pyroceramics, which can effectively protect the optical devices used in military equipment [15]. However, the developed materials are characterized by increased hardness and modulus of elasticity (Table 2), which does not correspond to such characteristics for natural teeth [16–18]. The low crack resistance of teeth is compensated by the presence of collagen both in their composition and when attaching them to the periodontium [19].

The increase in the crack resistance index for these materials is explained by the formation of nanoscale structure and crack blocking due to the structural rearrangement of the material during forming. Research indicates that a specific crystallographic orientation of LS_2 crystals contributes to a reduction in the variability of

the materials' elastic properties. This orientation results in an elastic modulus reaching up to 307 GPa, a compressive strength of 650 MPa, and an impact strength of as much as 5.5 kJ/mI. It was demonstrated that the formation of a closed-form mesh block structure by 0.4 μm LS_2 lamellar crystals results in a material with exceptional strength characteristics. Additionally, this material exhibits transparency within the visible light spectrum, enabling its application as a foundational component for the creation of transparent bulletproof pyroceramics, which can effectively protect the optical devices used in military equipment [15]. However, the developed materials are characterized by increased hardness and modulus of elasticity (Table 2), which does not correspond to such characteristics for natural teeth [16–18]. The low crack resistance of teeth is compensated by the presence of collagen both in their composition and when attaching them to the periodontium [19].

Therefore, the current task in creating a new type of glass-ceramic material for dental prosthetics is to ensure that their physicochemical properties match those of natural teeth and provide their long-term operation. This problem can be solved by developing nanostructured GCM based on lithium disilicate with increased fracture toughness under conditions of low-temperature rapid heat treatment.

2. EXPERIMENTAL PART

2.1. Setting the Aim and Research Methodology

The aim of the work is to study the structure formation of lithium-silicate glasses during the nucleation and crystal growth under conditions of rapid low-temperature heat treatment.

The study of phase transformations in glasses and the establishment of their heat treatment temperatures were carried out using electron microscopy (SEM Tesla 3 LMU with a resolution of 1 nm). The stress intensity coefficient of materials, K_{1C} [MPa·m$^{1/2}$], was determined by the calculation method [20], which was based on the measurement of the hardness of samples using a PMT-3.

2.2. Substantiation of the Choice of Compositions and Synthesis of Glasses for Obtaining Glass-Ceramic Materials

The selection of synthesis criteria is an important stage in predicting the composition of the initial glass matrix, which will provide the necessary performance properties of the glass-ceramic material in accordance with DIN EN ISO 13485.

Achieving the required mechanical and chemical properties of GCM for dentistry can be provided by forming a sitallized nano- and submicron structure of the glass matrix during heat treatment under the following conditions.

1. Fine-dispersed volume crystallization of glass under conditions of a three-stage low-temperature (< 800°C) rapid (< 1.5 h) heat-treatment regime due to:

— design of compositions based on lithium silicate glasses in the area of metastable liquation by the spinodal mechanism and crystallization of LS_2;

— ensuring the formation of stoichiometric groups $[SiO_4]^{4-}$ at a mass ratio of $SiO_2/Li_2O = 4.0$ to obtain a glass melt with a viscosity of more than 10^8 Pa·s for the formation of a significant number of lithium metasilicate nuclei;

— formation of a nanoscale sitallized structure with the formation of dendritic LS_2 crystals in a glass melt with a viscosity of more than 10^9 Pa·s.

2. Providing simultaneously a chemical and crack-resistant structure of the material with adjustable light transmission indicators by means of following phenomena and properties:

— a defined composition and content of the crystalline (80%) and chemically resistant glass phase;

— a specified content of particle sizes smaller than the wavelength in the visible part of the spectrum;

— correspondence of the refractive indices of the crystalline and glass phases;

— adjustment of optical scattering by changing the parameters of the heat treatment.

To obtain the glass-ceramic material, the previously synthesized SL-6 glass [20] was chosen with the following components, wt.%: Li_2O—15.0, LiF—2.5, Σ(MgO, ZnO)—4.0, Σ(TiO_2, ZrO_2)—5.0, Σ(CeO_2, MnO_2)—2.5, Σ(Al_2O_3, B_2O_3)—7.0, La_2O_3—2.0, P_2O_5—2.0, SiO_2—60.0, and $Li_2O/SiO_2 = 4$. The glass was synthesized under low-temperature melting conditions at a temperature of 1240°C.

To ensure the formation of hydroxyapatite (HA) crystals along with LS_2, CaO = 8 wt.% and P_2O_5 = 5 wt.% were added to the composition of SL 6 due to the exclusion of MnO_2, a decrease in the content of glass-forming components (Al_2O_3, B_2O_3) and oxides of RO and RO_2 group modifiers.

To ensure the formation of a significant number of nuclei, as a prerequisite for the formation of a fine-crystalline structure of the material, the ratio of crystallization catalysts $TiO_2/ZnO = 0.5–1.0$ was adjusted.

Experimental glasses SL 6.1 and SL 6.2 were obtained under identical melting conditions at temperatures of 1200–1250°C.

3. RESULTS AND DISCUSSION

3.1. Study of the Crystallization Character of Experimental Glasses during Heat Treatment

Studies of the crystallization character of the experimental glasses allowed us to establish a significant difference in the temperatures of appearance and growth of crystalline phases and their content. For the experimental glasses SL 6.1 and SL 6.2, a shift in the appearance of the first crystalline phase to the temperature range of 550°C is observed, which is a consequence of the phase separation at

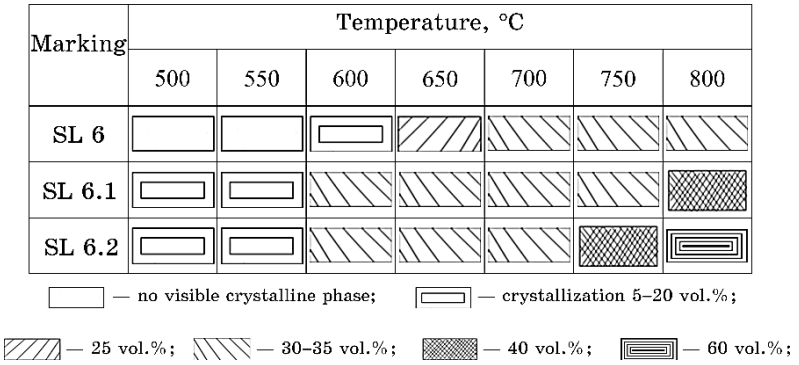

Fig. 2. Crystallization ability of experimental glasses after their heat treatment.

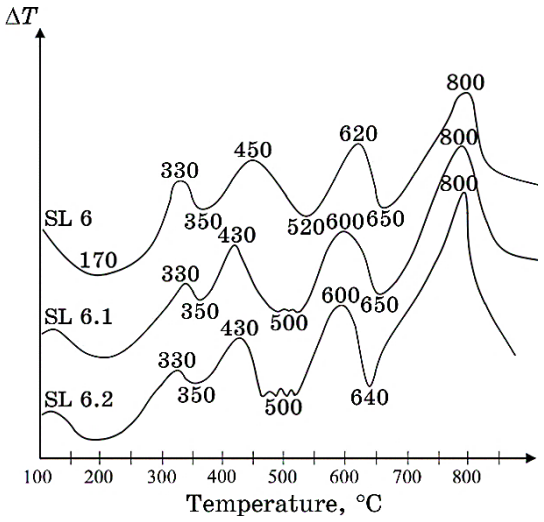

Fig. 3. Thermograms of experimental glasses.

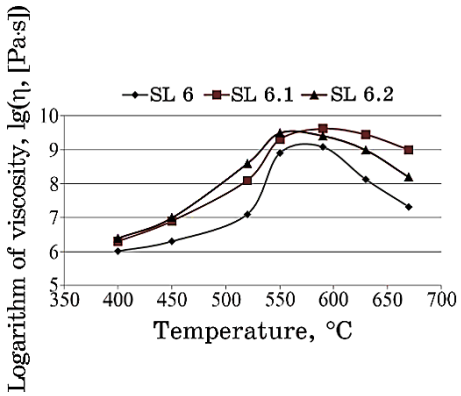

Fig. 4. Viscosity of experimental glasses.

500°C, which manifests itself as opalescence during prolonged exposure in a gradient furnace (Fig. 2) and is confirmed on the DTA curves as a slight alternating change in the slope of the curve in the temperature range of about 500°C (Fig. 3).

A characteristic feature of all the experimental glasses is an anomalous increase in viscosity within the glass-transition interval T_g–T_f (450–520°C), which is associated with the metastable liquation, which occurs under conditions of increased viscosity, and the formation of fluctuations. It is precisely due to the high viscosity of the glass that the formation of a developed droplet double-frame structure is observed in a short time (Fig. 4). Lowering the temperature to 620°C, at which an increase in crystallization viscosity $\eta > 10^9$ Pa·s is observed for the experimental glasses, leads to the fact that the glass automatically 'chooses' first those metastable crystalline phases that are most easily wetted by it and, as a result, are most strongly bound to it. The increase in viscosity for SL 6.2 glass when the temperature is lowered to 550°C allows for the intensification of the formation of nucleators for the growth of lithium metasilicate crystals, which are the basis for the subsequent crystallization of LS_2. In order to determine the optimal temperature of heat treatment for the formation of the dendritic structure of glass, the character of the formation of nuclei was investigated.

3.2. Study of the Formation Features of the Dendritic Structure of Experimental Glass at the Initial Stages

Dendrites are observed in a variety of crystalline materials, including snow minerals, casting alloys, chemicals, superalloys, and glass. These structures typically arise from diffusion-limited crystal

growth, resulting in intricate and often aesthetically pleasing tree-like formations. The theoretical frameworks, which describe dendritic growth, usually integrate principles of transport theory, encompassing heat conduction, melt convection, and species' diffusion, *i.e.*, areas, which are well established in the scientific community. In contrast, the microscopic interfacial phenomena involved, such as capillarity, molecular interface attachment, and viscosity-limited melt mobility, continue to be subjects of active research within the field of materials science.

A necessary condition for a strengthened crack-resistant structure is to ensure the dendritic crystallization in the glass structure by forming crystallites of a dendritic structure due to the attachment of atoms from the melt to the surface of the nucleus. In this case, the areas of the surface with a dense packing of atoms move into the melt at a lower speed than the areas of the surface with a low packing density. The shape of the crystal-melt interface depends on the temperature gradient near the crystallization front.

The dendritic structure is formed during accelerated or limited crystallization under non-equilibrium conditions, when the edges or vertices of the skeletal crystal are split according to certain laws [21, 22]. As a result, the crystalline structure of the object loses its initial integrity, and crystallographically ordered subunits appear.

The authors [15] studied the mechanism of dendritic crystal formation, the precursors of which branch and grow in the direction of the most intense mass transfer. Figure 5 shows the formation of the initial crystal based on the organization of the glass nanostructure (Fig. 5, *a*), the formation of spherulite groups according to crystallographic patterns (Fig. 5, *b*), the development from it of a LS_2 crystal of a clear pseudo-cubic habit in the form of crossed needles (Fig. 5, *c*) and the formation of a dendrite on its basis (Fig. 5, *d*).

To investigate the formation of LS_2 crystals in the structure of the experimental glass SL 6.2 during heat treatment, an area free from hydroxyapatite crystals was selected. According to the results of the study, the transformation of crystallization nuclei (Fig. 6, *a*), which were formed during glass melting, into spherocrystalline dendrites (Fig. 6, *b*) formed by branched dissymmetric spherocrystalline structures—spheroidolites, which form a unidirectional layered structure (Fig. 6, *c*) with the subsequent formation of LS_2 (Fig. 6, *d*).

This determines the possibility of further combining nanoscale spherulites into separate groups that interlock and determine the direction of dendrite crystallization. Dendrite formation occurs due to the intense release of latent heat of crystallization at the crystal boundary and a significantly supercooled glass melt, when a negative temperature gradient occurs that changes the mechanism of

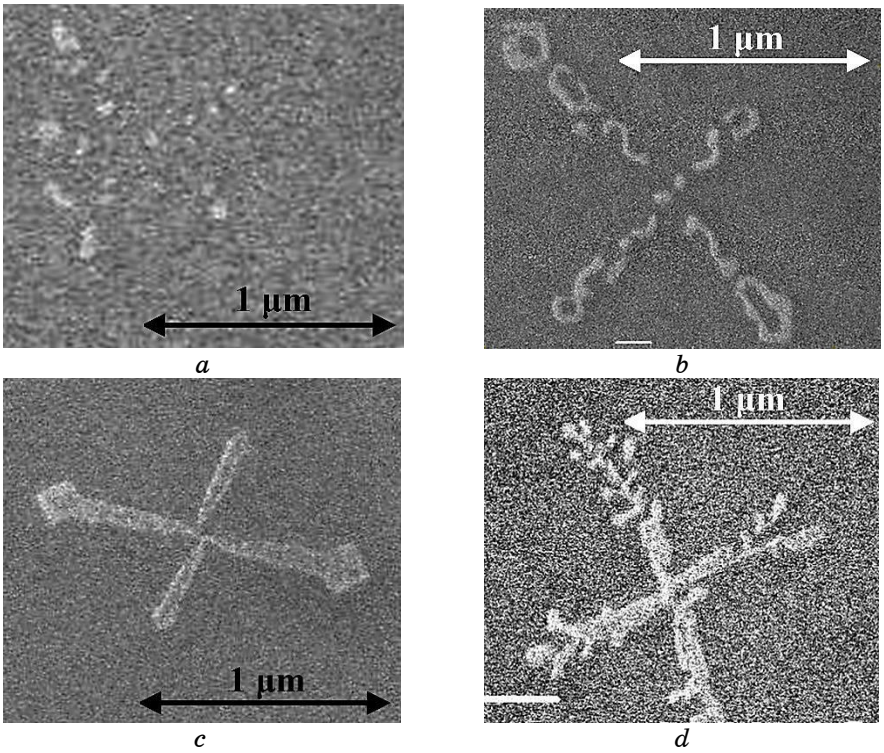

Fig. 5. Micrographs of LS_2 crystal formation in the structure of GCM [15] after melting (*a*) and after heat treatment at: (*b*) 630°C, (*c*) 820°C, (*d*) 850°C.

crystal growth. The further away from the boundary, the greater the melt supercooling. Therefore, any bulge on the surface of the nucleus falls into a zone of greater supercooling and grows deeper into the melt faster than flat surface areas, forming the primary elongated crystal axis.

An important condition for the effective limitation of crystal size by inhibiting the growth of spherulites at elevated temperatures is to ensure the phase separation of glass at high viscosity, which occurs in the region of 550°C. The tendency to phase separation is already evident after glass melting: nanoinhomogeneities of the structure, which are formed on the base of sybotaxic groups of crystals, are located in a directional manner in accordance with the crystallization front (Fig. 6, *a*). This determines the possibility of further combining nanoscale spherulites into separate groups that interlock and determine the direction of dendrite crystallization. Dendrite formation occurs due to the intense release of latent heat of crystallization at the crystal boundary and a significantly super-

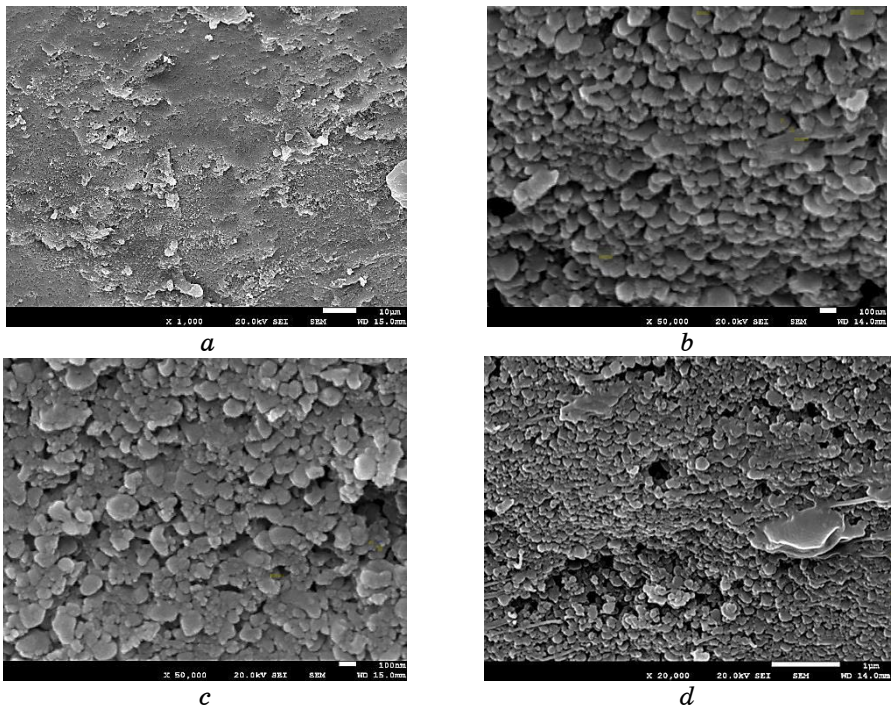

Fig. 6. Photomicrographs of experimental glass SL 6.2 after melting (*a*) and after heat treatment at: (*b*) 550°C, (*c*) 600°C, (*d*) 800°C.

cooled glass melt, when a negative temperature gradient occurs that changes the mechanism of crystal growth. The further away from the boundary, the greater the melt supercooling. Therefore, any bulge on the surface of the nucleus falls into a zone of greater supercooling and grows deeper into the melt faster than flat surface areas, forming the primary elongated crystal axis.

Formation of dendritic nano- and submicron structure of GCM based on lithium disilicate is determined by the possibility of following phenomena and properties:

— the metastable phase separation in the nucleation region ($T = 550$°C);

— high viscosity $\eta > 10^9$ Pa·s in the area of nucleation and crystal growth;

— ensuring self-organization of the spherulite structure ($T = 600$°C);

— the formation of a branched layered dendritic structure with a crystal size of 0.4–1.0 μm ($T = 800$°C).

Taking into account the studies of the crystallization ability, the following heat treatment regime was chosen: annealing—430°C, 30

TABLE 3. Characteristics of the phase composition and properties of the developed GCM.

Marking	Characteristics of crystalline phases		Properties			
	type	content, vol.%	*HV*, GPa	K_{1C}, MPa·m$^{1/2}$	*E*, GPa	ρ, g/cm^3
SL 6	LS_2 β-SP	80	8.28	3.00	93	2400
SL 6.1	LS_2 HA	80	7.50	3.50	100	2350
SL 6.2	LS_2 HA	80	7.50	5.00	130	2350

min; firing at I stage—600°C, 30 min, at II stage—800°C, 30 min.

3.3. Study of the Properties GCM

The optimized GCM SL 6.1 and SL 6.2 are characterized by increased fracture toughness (Table 3), which can significantly increase its service life by means of the reinforcement of the sitallized nanomaterial and the ability to self-heal *in vivo*, which is typical for biomimetic materials [23].

Reduced indicators of density and hardness, modulus of elasticity make it possible to bring the properties of the developed materials closer to those of natural teeth (Tables 2, 3). A decrease in the heat resistance of the developed materials in comparison with IPS e.max CAD (Table 2) eliminates the cracking of the material during its heat treatment, and an increase in chemical resistance ensures its durability.

4. CONCLUSIONS

The main types of dental materials and the features of their application were analysed with regard to their properties. The prospects for the use of GCM have been established, given their high operational properties, manufacturability and reduced cost compared to ceramic dental prostheses. The advantages of using GCM based on LS_2 and ways to improve their structure and properties have been determined, as well as the main criteria for ensuring the sitallized nano- and submicron structure of the glass matrix under conditions of low-temperature heat treatment in order to form a strengthened chemically resistant structure of the material with increased fracture toughness and adjustable light transmission indicators. The composition of lithium silicate glasses with a ratio of $Li_2O/SiO_2 = 4$ was developed and modified by adding $CaO = 8$ wt.% and $P_2O_5 = 5$

wt.% due to the exclusion of MnO_2, reducing the content of glass-forming components (Al_2O_3, B_2O_3) and oxides of RO and RO_2 group and the ratio of crystallization catalysts $TiO_2/ZnO = 0.5–1.0$ is ensured for the formation of a fine-crystalline structure of the material. The mechanism of phase formation in glasses has been determined, which consists in the formation of a sitallized nanostructure of glass due to intensive self-organization of spherulites and the formation of lithium metasilicate nucleators (550°C, $\eta = 10^{9.5}$ Pa·s) with a size of 50–100 nm, the growth of which is limited due to the phase separation of the glass; the formation of spherocrystalline dendrites of lithium metasilicate (600°C) with the subsequent formation of a branched layered dendritic structure of LS_2 crystals with a size of 0.4–1.0 μm ($T = 800$°C) against the background of dense packing of spheroidolites. The formation of a dissipative structure at the initial stages of nucleation allows for accelerated sitallization under conditions of limiting crystal size growth.

Technological parameters for obtaining strengthened GCM based on lithium disilicate for dental purposes (annealing—450°C, 30 min; firing—600°C, 30 min; 800°C, 30 min) necessary for the formation of a fine-crystalline interlocked nanostructure with the presence of the main crystalline phase of LS_2 with a total content crystalline phases of 80 vol.% have been determined.

According to the results of the conducted studies, the possibility of obtaining competitive dental materials in accordance with DIN EN ISO 13485 with increased fracture toughness $K_{1C} = 5.0$ MPa·m$^{1/2}$ has been established.

REFERENCES

1. L. Vaiani, A. Boccaccio, A. E. Uva, G. Palumbo, A. Piccininni, P. Guglielmi, S. Cantore, L. Santacroce, I. A. Charitos, and A. Ballini, *J. Funct. Biomater.*, **14**, No. 3: 146 (2023); https://doi.org/10.3390/jfb14030146
2. H. Y. Shi, R. Pang, J. Yang, D. Fan, H. Cai, H. B. Jiang, J. Han, E. S. Lee, and Y. Sun, *Biomed. Res. Int.*, **2022**, No. 1: 8451445 (2022); https://doi.org/10.1155/2022/8451445
3. A. Warreth and Y. Elkareimi, *Saudi Dent. J.*, **32**, No. 8: 365 (2020); https://doi.org/10.1016/j.sdentj.2020.05.004
4. C. G. Soubelet, C. A. Grillo, G. Suárez, and F. M. Stabile, *Ceram. Int.*, **50**, No. 9, Pt. A: 14347 (2024); https://doi.org/10.1016/j.ceramint.2024.01.346
5. S. Kongkiatkamon, D. Rokaya, S. Kengtanyakich, and C. Peampring, *Peer J.*, **11**, No. 2: e15669 (2023); https://doi.org/10.7717/peerj.15669
6. S. Ban, *Materials*, **14**, No. 17: 4879 (2021); https://doi.org/10.3390/ma14174879
7. S. Ahmed, M. Zhang, V. Koval, L. Zou, Z. Shen, R. Chen, B. Yang, and H. Yan, *J. Am. Ceram. Soc.*, **105**, No. 2: 1106 (2022); https://doi.org/10.1111/jace.18139

8. G. A. Khater and E. M. Safwat, *J. Non-Cryst. Solids*, **563**: 120810 (2021); https://doi.org/10.1016/j.jnoncrysol.2021.120810
9. M. S. Dahiya, V. K. Tomer, and S. Duhan, *Woodhead Publishing Series in Biomaterials Applications of Nanocomposite Materials in Dentistry* (Eds. A. M. Asiri, Inamuddin, and A. Mohammad) (Woodhead Publishing: 2019), p. 1–25; https://doi.org/10.1016/B978-0-12-813742-0.00001-8
10. F. Soleimani, H. A. Babaei, and M. Soleimani, *Ceram. Int.*, **48**, No. 15: 22545 (2022); https://doi.org/10.1016/j.ceramint.2022.04.172
11. K. Li, H. Kou, and C. Ning, *J. Non-Cryst. Solids*, **552**: 120443 (2021); https://doi.org/10.1016/j.jnoncrysol.2020.120443
12. S. Brandt, A. Winter, H.-C. Lauer, F. Kollmar, S.-J. Portscher-Kim, and G. E. Romanos, *Materials*, **12**, No. 3: 462 (2019); https://doi.org/10.3390/ma12030462
13. B. de F. Vallerini, L. D. Silva, M. de O. C. Villas-Bфas, O. P. Filho, E. D. Zanotto, and L. A. P. Pinelli, *Ceram. Int.*, **50**, No. 1: 188 (2024); https://doi.org/10.1016/j.ceramint.2023.10.093
14. O. V. Savvova, G. K. Voronov, V. L. Topchiy, and Yu. O. Smyrnova, *Chemistry & Chemical Technology*, **12**, No. 3: 391 (2018); https://doi.org/10.23939/chcht12.03.391
15. O. V. Savvova, V. L. Topchyi, O. V. Babich, and R. O. Belyakov, *Strength. Mater.*, **50**, No. 2: 874 (2019); https://doi.org/10.1007/s11223-019-00034-3
16. Y. R. Zhang, W. Du, X. D. Zhou, and H. Y. Yu, *Int. J. Oral. Sci.*, **6**, No. 2: 61 (2014); https://doi.org/10.1038/ijos.2014.21
17. K. Chu, C. Zhao, and F. Ren, *Biosurface and Biotribology*, **7**, No. 4: 228 (2021); https://doi.org/10.1049/bsb2.12022
18. K. Sarna-Boś, K. Skic, P. Boguta, A. Adamczuk, M. Vodanovic, and R. Chałas, *Micron*, **172**: 103485 (2023); https://doi.org/10.1016/j.micron.2023.103485
19. S. P. Ho, S. J. Marshall, M. I. Ryder, and G. W. Marshall, *Biomaterials*, **28**, No. 35: 5238 (2007); https://doi.org/10.1016/j.biomaterials.2007.08.031
20. O. Savvova, O. Babich, M. Kuriakin, A. Grivtsova, and V. Topchiy, *Functional Material*, **24**, No. 3: 1 (2017); https://doi.org/10.15407/fm24.02.311
21. M. E. Glicksman, *Handbook of Crystal Growth* (Eds. T. Nishinaga) (Waltham, MA, USA: 2015), p. 669; https://doi.org/10.1016/B978-0-444-56369-9.00016-2
22. A. Ayyagari, V. Hasannaeimi, H. Arora, and S. Mukherjee, *Sci. Rep.*, **8**: 906 (2018); https://doi.org/10.1038/s41598-018-19488-7
23. S. Hossain and N. M. Ravindra, *TMS-2019 148th Annual Meeting & Exhibition Supplemental Proceedings* (2019), p. 1643; https://doi.org/10.1007/978-3-030-05861-6_153